



HAL
open science

Efficient Resolution of Metastatic Tumour Growth Models by Reformulation into Integral Equations

Niklas Hartung

► **To cite this version:**

Niklas Hartung. Efficient Resolution of Metastatic Tumour Growth Models by Reformulation into Integral Equations. 2014. hal-00935233

HAL Id: hal-00935233

<https://hal.science/hal-00935233>

Preprint submitted on 23 Jan 2014

HAL is a multi-disciplinary open access archive for the deposit and dissemination of scientific research documents, whether they are published or not. The documents may come from teaching and research institutions in France or abroad, or from public or private research centers.

L'archive ouverte pluridisciplinaire **HAL**, est destinée au dépôt et à la diffusion de documents scientifiques de niveau recherche, publiés ou non, émanant des établissements d'enseignement et de recherche français ou étrangers, des laboratoires publics ou privés.

Efficient Resolution of Metastatic Tumour Growth Models by Reformulation into Integral Equations

Niklas Hartung

Aix-Marseille Université, CNRS, Centrale Marseille, LATP, UMR 7353

39, rue F. Joliot Curie, 13453 Marseille Cedex 13, FRANCE

niklas.hartung@univ-amu.fr

Tel. +33 699590027

Abstract

The McKendrick/Von Foerster equation is a transport equation with a non-local boundary condition that appears frequently in structured population models. A variant of this equation with a size structure has been proposed as a metastatic growth model by Iwata *et al.*

Here we will show how a family of metastatic models with 1D or 2D structuring variables, based on the Iwata model, can be reformulated into an integral equation counterpart, a Volterra equation of convolution type, for which a rich numerical and analytical theory exists. Furthermore, we will point out the potential of this reformulation by addressing questions coming up in the modelling of metastatic tumour growth. We will show how this approach permits to reduce the computational cost of the numerical resolution and to prove structural identifiability.

1 Introduction

The organism-scale nature of cancer is a major challenge for clinical oncology. As long as the disease is spatially confined, it can often be cured by a local intervention, but once a cancer metastasises, the prognostic deteriorates rapidly. Another major difficulty is that small metastases are often invisible on medical images, such that the metastatic state of a patient is only known with certainty once the metastatic growth has already advanced. A better knowledge of a patient's metastatic state therefore has a major clinical importance, permitting, for example, a more targeted drug administration.

Approaches combining biomedical studies with mathematical modelling have recently been more and more recognised as powerful tools driving preclinical and clinical cancer research. For the description of metastatic growth, mathematical models have a potential to estimate the metastatic state in situations

where it cannot be seen on medical images. Ultimately, based on biomarker information, a set of model parameters could be determined for each patient to predict the metastatic state and evolution in an individual manner. Being recognised as a key step in the evolution of cancer, metastatic emission and growth has been modelled by different techniques, covering phenomenological and mechanistic, deterministic and stochastic models. For a recent overview on modelling of the metastatic process, we refer to the review by Scott *et al.* [24]. For the biology of metastasis, the reviews by Gupta and Massagué [11] and by Chaffer and Weinberg [9] are excellent reading.

As a preliminary validation step of a mathematical model, the model dynamics has to be able to reproduce the metastatic growth in preclinical experiments. Typically, the statistical parameter estimation needed for this validation step requires a large number of model simulations. Therefore, efficient model simulation is fundamental, which makes structurally simple phenomenological models particularly suitable for this type of model validation.

The so-called McKendrick/Von Foerster equation, introduced independently by McKendrick [21] and 30 years later by Von Foerster [27], is a partial differential equation (PDE) for the description of the evolution of an age-structured population with a non-local boundary condition. Since then, the McKendrick/Von Foerster equation has been taken up, analysed and extended in numerous publications. We refer to a monograph by Perthame [22] containing a mathematical analysis of structured population models including the McKendrick/Von Foerster equation and extensions thereof.

A particular variant of the McKendrick/Von Foerster equation has been introduced by Iwata *et al.* [19] to model metastatic growth. The *Iwata model* has been shown to describe the metastatic growth dynamics visible on CT scans of a patient attained by a metastatic hepatocellular carcinoma very accurately. It has further been shown that the model can be calibrated to reproduce the risk of a metastatic disease given a certain primary tumour size [3].

In a work by Barbolosi *et al.* [2], the model has been extended to include the effect of a chemotherapy and an efficient numeric resolution scheme has been proposed. Another important model extension is due to Benzekry [4, 6], who established the theory for a model version featuring a two-dimensional structuring variable in order to take a combined chemotherapy/antiangiogenic therapy into account. Finally, a model formulation distinguishing between different metastatic generations was discussed by Devys *et al.* [10].

The numerical resolution of these models is not without difficulties: several authors have described problems arising when using typical PDE schemes due to large scale differences in model dynamics for biologically relevant parameters [2, 10, 6]. Furthermore, it comes at a considerable computational cost, particularly in the 2D case. Using methods reported in the literature, the computational cost quickly becomes limiting in statistical parameter estimation, where a large number of model simulations is needed. This obstacle has been emphasised at several occasions [17, 25].

In this article, we will present a model reformulation into Volterra integral equations, which have been thoroughly studied since the beginning of the 20th

century [20]. This reformulation will permit a considerable acceleration and improved accuracy of the numerical model resolution because there exists an ample variety of techniques for the efficient resolution of the Volterra integral equations of convolution type (see, for example, the review by Baker [1]). The basic technique used for this reformulation has already been described by Ianelli [18], although only in the 1D age-structured case for the number of metastases. In the case of size-structured models or in 2D, a change of variables used by Benzekry [6] could be described as the first step of the reformulation into a Volterra equation. To the best of the author’s knowledge, a general framework covering 2D structuring variables and for arbitrary observables has not been proposed yet. Also, the advantage of the reformulation in terms of a more efficient numerical resolution of the PDE model has not been described so far. Indeed, whenever the numerical resolution of the Iwata model is discussed in the literature, the proposed methods are based on the PDE formulation of the model [2, 10, 6].

Outline. The article is structured as follows. In Chapter 2, the 1D and 2D metastatic models are presented, as well as the biological *observables*, which are not the metastatic density function itself but rather weighted integrals of this density. Furthermore, the *characteristic* or *semi-Lagrangian* scheme is introduced, which is used by Barbolosi *et al.* ([2] and [26]) for the numerical resolution of these models. In Chapter 3, the 1D and 2D models are reformulated into Volterra integral equations and the numerical resolution of the reformulated model is sketched. In a particular case of the 1D model, a result on structural identifiability is obtained. In Chapter 4, the numerical resolution methods based on the PDE and on the Volterra integral equation are compared in terms of efficiency. First, in a theoretical part, we show heuristically how the numerical resolution is improved in case of the integral equation. Then, numerical results are presented for the 1D and 2D models comparing the model performances. In Chapter 5, extensions (non-zero initial data, Dirac-type observable) and limitations (non-autonomous growth rates) of the reformulation are discussed.

Note that this article is not meant as an in-depth discussion of the advantages and drawbacks of the modelling approach. In a recent work [16], the techniques described in this article are used for model building based on preclinical data and the adequacy of the modelling approach is discussed in detail.

2 The metastatic models formulated as PDE

2.1 The 1D metastatic model

2.1.1 Model description

Iwata *et al.* [19] introduced a model for metastatic growth, describing the evolution of metastases at the organism-scale by means of a structured population equation: Primary tumour growth is described by an ODE model $x_p' = g(x_p)$ (Eq. 1), which is typically a function $g(x) = xh(x)$ with decreasing h , such as

the Gompertz function $g(x) = ax \log(b/x)$. Metastatic growth is described by a transport equation: a density function “is transported in size” at rate g (Eq. 2). Metastatic emission is modelled by a non-linear boundary condition (Eq. 3): both primary tumour and metastases emit metastases at a rate β depending on their size. It is supposed that newborn metastases are monocellular. It is further assumed that no metastases are present at time $t = 0$ (Eq. 4). For a schematic overview of the mechanisms represented in the model, see also Figure 1, and for model derivation, see [19].

$$x_p(t)' = g(x_p(t)), \quad x_p(0) = x_0, \quad t \in [0, +\infty), \quad (1)$$

$$\partial_t \rho(x, t) + \partial_x [g(x) \rho(x, t)] = 0, \quad (x, t) \in (1, b) \times (0, +\infty), \quad (2)$$

$$g(1) \rho(1, t) = \beta(x_p(t)) + \int_1^b \beta(x) \rho(x, t) dx, \quad t \in (0, \infty), \quad (3)$$

$$\rho(x, 0) = 0, \quad x \in [1, b]. \quad (4)$$

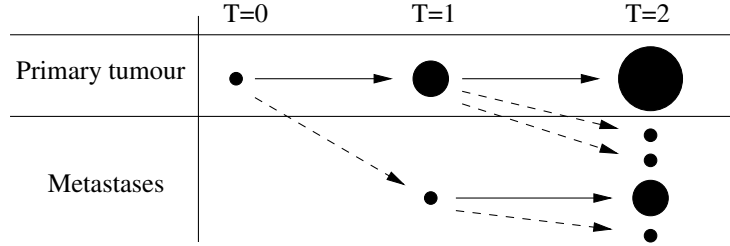


Figure 1: *Schematic representation of the main phenomena in model (1-4). Solid lines represent growth at rate $g(x)$ and dashed lines represent emission at rate $\beta(x)$. At time $T = 0$, only the primary tumour is present and consists of one cell. At time $T = 1$, the primary tumour has grown and has emitted a metastasis which is born with initial size $x_0 = 1$. At time $T = 2$, the primary tumour has grown further and now emits metastases at a rate faster than at $T = 1$ (the rate $\beta(x)$ is increasing in x). Also, the metastasis that has been created before $T = 2$ has grown and emits metastases itself.*

Iwata *et al.* used clinical data from a patient afflicted with a hepatocellular carcinoma to estimate the parameters in the following parametrised model:

$\beta(x) = mx^\alpha$. The emission rate is supposed to be proportional to a power of the number of cells.

$g(x) = ax \log(b/x)$. Primary and secondary tumour growth is modelled by the same Gompertz function.

$x_p(0) = 1$. The primary tumour is initiated from a single cell.

The hypothesis that primary and secondary tumours follow the same growth dynamics can be attributed to the fact that both primary tumour and metastases are localised in the same organ in the clinical case used by Iwata *et al.* , but it might be unreasonable in other scenarios. For an animal model with xenografted tumour cells, the assumption $x_p(0) = 1$ should also be revised. These assumptions can easily be dropped, however (see Remark 1 for the general framework of the analysis).

It has further been shown by Barbolosi *et al.* [3] that the model can be calibrated to reproduce the results of a clinical study on breast cancer relating the risk of a metastatic disease to the primary tumour size.

The Iwata model has been taken up and analysed or extended in a considerable number of publications. Notably, a thorough mathematical analysis of the model, including a numeric resolution scheme and an extension that permits to model the action of a chemotherapy, has been performed by Barbolosi *et al.* [2]. The main difference in the model extension for therapeutic action is a non-autonomous growth function $g(x, t)$. We will discuss the reformulation technique in this case in Chapter 5.

Both the analysis and the numerical resolution of the model make extensive use of the notion of *characteristic curves*, which are the solutions $Y(t; t_0, x_0)$ of

$$\frac{dY}{dt}(t; t_0, x_0) = g(Y(t; t_0, x_0)), \quad Y(t_0; t_0, x_0) = x_0. \quad (5)$$

We will come back to this issue when discussing the numerical resolution of Eqs. (1-4). Among the characteristic curves, the curve

$$X(t) := Y(t; 0, 1) \quad (6)$$

has a particular role because it separates the characteristics coming from the boundary ($x = 1$) from those coming from the initial condition ($t = 0$).

Remark 1 (General setting). *The reformulation proposed in this article can be performed for the more general model*

$$\begin{aligned} \partial_t \rho(x, t) + \partial_x [g(x) \rho(x, t)] &= 0, \\ g(1) \rho(1, t) &= S(t) + \int_1^b \beta(x) \rho(x, t) dx, \\ \rho(x, 0) &\equiv \Phi(x), \end{aligned} \quad (7)$$

assuming $S \in C^1([0, T])$, $\Phi \in C^1([1, b])$ with $\Phi(b) = 0$, $g \in C^1([1, b])$ positive with $g(b) = 0$. This setting notably covers the case of different growth and emission rates of primary and second tumours with $S(t) = \beta_p(x_p)$, where the primary tumour emission function β_p can be different from β and the primary tumour growth can be modelled by a law other than (1).

In Chapters 2 through 4, the particular case (1-4) is discussed for an easier presentation. In Chapter 5 we will discuss how the reformulation can be done in the general case (7).

Remark 2 (Biological observables in the 1D model). *In many cases, the quantity of interest is not the metastatic density ρ , but rather a biological observable. This is particularly the case when the model is used to confront predictions to preclinical or clinical data. These observables can generally be written as weighted integrals of the metastatic density:*

$$F_f(t) := \int_1^b f(x)\rho(x,t)dx. \quad (8)$$

Let us give some examples of observables written in this way:

Total number of metastases. $f(x) \equiv 1$

Cumulative number of metastases. $f(x) \equiv \chi_{x \geq c}(x)$. *In Iwata et al. [19], parameters are estimated from what they called the cumulative number of metastases, that is, the number of metastases greater than a certain size c ($F_f(t) = \int_c^b \rho(x,t)dx$).*

Metastatic mass. $f(x) = x$. *The metastatic mass is the total biomass of all the metastases put together. Along with the number of metastases, it is the main observable available in quantitative imaging.*

Rate of metastatic birth. “ $f(x) = \delta_1(x)$ ”. *Although only formally written in the form (8), the rate of metastatic birth can also be formulated as the solution of a Volterra integral equation (see Chapter 5 for a rigorous discussion of this observable). The rate of metastatic birth is not a real biological observable, but it can be used to compute the whole metastatic density function, which could be of interest in theoretical studies.*

Remark 3 (Regularity of solutions). *In general, Eqs. (7) only have a weak solution $\rho \in C([0, T], L^1(1, b))$. It solves Eqs. (7) in a classical sense only if the following compatibility condition between the initial condition and the boundary condition is satisfied (see Barbolosi et al. [2]):*

$$g(1)\Phi(1) = S(0) + \int_1^b \beta(x)\Phi(x)dx. \quad (9)$$

The reformulations in the following section are to be understood as follows. The calculations are performed in a regular setting of strong solutions, for approximated source terms S_n satisfying the compatibility condition, to obtain the integral equation for an approximate observable F_f^n . Then, passing to the limit $S_n \rightarrow S$, the integral equation is obtained for the observable F_f that we are interested in. Because of the structure of F_f as an integral of ρ weighted with a L^∞ -function, the weak L^1 -convergence $\rho_n \rightharpoonup \rho$ that has been shown by Barbolosi et al. [2] is sufficient.

2.1.2 Numerical resolution of the 1D model

Typical numerical schemes for hyperbolic PDEs, such as the upwind-scheme, perform badly in solving Eqs. (1-4). This is mainly due to the large scale differences coming up in the dynamics of the model when taking biologically relevant parameters. With the model parameters that Iwata *et al.* [19] have estimated from clinical data, the sizes of newly emitted metastases and that of early metastases differ in up to 10 orders of magnitude, making an uniform discretisation of the metastatic size unrealistic. One could resort to high-order schemes with a logarithmic size discretisation, but they are still time-consuming in model resolution.

The characteristic scheme, which has been proposed by Barbolosi *et al.* [2] for the resolution of Eqs. (1-4), overcomes these difficulties and permits a faster resolution. The starting point of this scheme is the fundamental property of the transport equation, a conservation relation along the characteristic curves (5):

$$\frac{d}{dt}(g(Y(t; t_0, x_0))\rho(Y(t; t_0, x_0), t)) = 0. \quad (10)$$

While the time interval $[0, T]$ is uniformly discretised ($t_n = \frac{nT}{N}$), the size variable is now discretised according to the characteristic curve (6): $x_n = X(t_n)$. Note that since (5) is autonomous,

$$Y(t_n; t_i, x_j) = X(t_{n-i+j}).$$

This discretisation allows to exploit the conservation relation (10) for the calculation of an approximation $\rho_{i,k}$ of $\rho(x_i, t_k)$ because

$$g(x_i)\rho_{i,k} = g(x_{i-1})\rho_{i-1,k-1}$$

holds. The full scheme is given by

$$\begin{aligned} \rho_{i,k} &= \frac{g(x_{i-1})}{g(x_i)}\rho_{i-1,k-1} && \text{for } k \geq i > 0, \\ g(1)\rho_{0,k} &= \beta(x_p(t_k)) + Q((\beta(x_i)\rho_{i,k})_{i=1}^N) && \text{for } k > 0, \\ \rho_{i,k} &= 0 && \text{for } k < i. \end{aligned} \quad (11)$$

The second line comes from the fact that we assumed a zero initial condition. The integral quadrature could be a rectangle or a trapezoidal rule. The observable is then calculated as

$$F_f(t_k) = Q((f(x_i)\rho_{i,k})_{i=1}^N).$$

The characteristic scheme only involves an approximation in the integral quadrature – along the characteristic curves, it is exact.

2.2 Metastatic generations in the 1D model

In model (1-4), a generational structure is implicitly contained: the metastatic density function ρ can be decomposed into a sum $\sum_{k=0}^{\infty} \rho^k$, where ρ^0 denotes the

metastases emitted directly by the primary tumour, ρ^1 the metastases emitted from the metastases emitted from the primary tumour, *et cetera*. In mathematical terms, the metastatic generation ρ^0 is solution of

$$\begin{aligned}\frac{\partial}{\partial t}\rho^0(x, t) + \frac{\partial}{\partial x}[g(x)\rho^0(x, t)] &= 0, \\ g(1)\rho(1, t) &= \beta(x_p(t)), \\ \rho^0(\cdot, 0) &\equiv 0.\end{aligned}\tag{12}$$

and for $k > 0$, ρ^k is solution of

$$\begin{aligned}\frac{\partial}{\partial t}\rho^k(x, t) + \frac{\partial}{\partial x}[g(x)\rho^k(x, t)] &= 0, \\ g(1)\rho^k(1, t) &= \int_1^b \beta(x)\rho^{k-1}(x, t)dx, \\ \rho^k(\cdot, 0) &\equiv 0.\end{aligned}\tag{13}$$

Analytical and numerical aspects of metastatic generations in the PDE model have been discussed by Devys *et al.* [10]. An important point to note is that different generations arise at different times. Whereas $\rho \approx \rho^0$ for small times, the other metastatic generations appear one after another for bigger times, and the asymptotic behaviour $\lim_{t \rightarrow +\infty} \rho(\cdot, t)$ is determined by all generations together. For small and medium observation times, however, a very close approximation of the full model is obtained when taking only the first few metastatic generations into account.

2.3 The 2D metastatic model

The two-dimensional metastatic model (14) was introduced by Benzekry [4] as an extension of the *Iwata* model in order to take into account a combined chemotherapy/antiangiogenic therapy. The particular case studied in that work was a structure in size and vascular capacity, modelled by an ODE model by Hahnfeldt *et al.* [13]. The analysis was performed in a general setting, however. Other structures, such as two cellular subpopulations (e.g. dividing and non-dividing cells, based on a model by Gyllenberg and Webb [12]), could also be modelled in the 2D framework (the case of dividing and nondividing cells will be considered in [15]).

$$\begin{aligned}X_p(t)' &= G(X_p(t)), \quad X_p(0) = X_0 && \text{with } X_0 \in \Omega \subset \mathbb{R}^2, \\ \partial_t \rho(X, t) + \text{div}[G(X)\rho(X, t)] &= 0 && \forall (t, X) \in (0, T) \times \Omega, \\ G(\sigma)\rho(\sigma, t) &= b(X_p(t), \sigma) + \int_{\Omega} b(X, \sigma)\rho(X, t)dX && \forall t \in (0, T), \forall \sigma \in \partial\Omega \\ \rho(X, 0) &\equiv 0 && \forall X \in \Omega.\end{aligned}\tag{14}$$

Conditions on G are needed to ensure the existence of solutions (which are fulfilled for the Hahnfeldt and Gyllenberg-Webb models). To remain as simple as possible, we will not include the details and refer to Benzekry [5] for that discussion.

A crucial hypothesis for the analysis of model (14) performed by Benzekry is that the trait of newly born metastases be independent of that of the tumour which emitted them:

$$b(X, \sigma) = N(\sigma)\beta(X). \quad (15)$$

Similar to (10), a conservation property along characteristic curves also holds in the 2D case. In the following, this is stated in an abbreviated way (see Benzekry [6] for a more detailed version). The characteristic curves are given by

$$\begin{aligned} Y'(t; t_0, \sigma) &= G(Y(t; t_0, \sigma)), \\ Y(t_0; t_0, \sigma) &= \sigma, \end{aligned} \quad (16)$$

and we will make particular use of $X(t; \sigma) := Y(t; 0, \sigma)$. The conservation property is now formulated using the Jacobi determinant J_Φ of the map $\Phi : (t, \sigma) \rightarrow X(t; \sigma)$. The Jacobi determinant J_Φ can be characterised as the solution of

$$\begin{aligned} \partial_t J_\phi(t, \sigma) &= \text{div}(G(X(t; \sigma)))J_\phi(t, \sigma), \\ J_\Phi(t_0, \sigma) &= G \cdot \nu(\sigma), \end{aligned}$$

and the conservation property is then given by

$$\frac{d}{dt} (\rho(X(t; \sigma), t)J_\Phi(t, \sigma)) \equiv 0. \quad (17)$$

Remark 4 (Biological observables in the 2D model). *In the 2D model, the observables are given by*

$$F_f(t) = \int_{\Omega} f(x, y)\rho(x, y, t)dx dy.$$

As in the 1D case, the total number of metastases is given by $f(x, y) \equiv 1$. However, in contrast to the 1D model, where the structuring variable is always the size, the interpretation of other observables $F_f(t)$ in the 2D model will depend on the nature of the structuring variables (x, y) . For example, if x is the size and y is an additional trait of the metastases, the metastatic mass will be given by $f(x, y) = x$. On the other hand, if x and y are two complementary cellular subpopulations (such as dividing and non-dividing cells), the metastatic mass will be given by $f(x, y) = x + y$. In the latter case, the total volume of the subpopulations ($f(x, y) = x$ and $f(x, y) = y$, respectively) could also be of interest.

For a detailed presentation of the numerical resolution by the characteristic scheme in the 2D case, we refer to Benzekry [6].

3 Model reformulations into integral equations

3.1 1D model

3.1.1 Reformulation

In this section, we will present the reformulation of the model (1-4) into a Volterra integral equation of convolution type. The reformulation will be done for the *model observables* $F_f(t) = \int_1^b f(x)\rho(x,t)dx$. As previously said, biologically observable quantities can generally be written in this way. Note that in view of Remark 3, we can obtain the integral equation working with the strong solutions of the metastatic model.

Theorem 1. *Let ρ be the solution of (1-4), x_p the primary tumour size and X the characteristic curve that solves Eq. 6. Then, the observable $F_f(t)$ defined in (8) solves the **Volterra equation of the second kind of convolution type***

$$F_f(t) = [f(X) * \beta(x_p)](t) + [\beta(X) * F_f](t). \quad (18)$$

Remark 5 (Explanation of the convolution structure). *If we neglect the metastatic emission by the metastases themselves (in other words, considering only the first metastatic generation), only the first term in (18) remains, that is,*

$$F_f(t) = [f(X) * \beta(x_p)](t).$$

Looking at this expression, it can easily be understood why the convolution structure appears. The metastases are emitted at rate $\beta(x_p)$ and grow at a rate X . Thus, at time t , a metastasis emitted at time $s < t$ will grow during the time interval $t - s$, and the total observable is given by integrating over all possible emission times, yielding the convolution.

Proof. The first step in reformulating problem (1-4) consists of a change of variables that will permit to exploit the conservation property (10) by following back the characteristic curve until the boundary condition. Writing $x = X(s)$, $dx = X'(s)ds = g(X(s))ds$, we have

$$\begin{aligned} F_f(t) &= \int_1^{X(t)} f(x)\rho(x,t)dx = \int_0^t f(X(s))g(X(s))\rho(X(s),t)ds \\ &\stackrel{(10)}{=} \int_0^t f(X(s))g(1)\rho(1,t-s)ds \\ &\stackrel{(3)}{=} \int_0^t f(X(s)) \left[\beta(x_p(t-s)) + \int_1^b \beta(x)\rho(x,t-s)dx \right] ds \\ &= f(X) * (\beta(x_p) + F_\beta)(t). \end{aligned} \quad (19)$$

For the observable F_β , (19) yields the following equation:

$$F_\beta(t) = \beta(X) * (\beta(x_p) + F_\beta)(t).$$

This can now be used to obtain (18) for F_f with arbitrary f . Starting from (19), we calculate

$$\begin{aligned} F_f &= f(X) * (\beta(x_p) + F_\beta) \\ &= f(X) * \beta(x_p) + f(X) * [\beta(X) * (\beta(x_p) + F_\beta)] \\ &= f(X) * \beta(x_p) + \beta(X) * F_f. \end{aligned}$$

□

3.1.2 Application: structural identifiability

As we will see in the following, the previous reformulation will permit an efficient calculation of the observable quantities. In addition to that, in the particular case that primary and secondary tumours grow at the same speed, we can also use it to obtain a structural identifiability result.

Corollary 1 (Structural identifiability). *Let $x_p \equiv X$ with X defined as in (6). If $f \in C^1$ with $f(X(0)) \neq 0$, then β is identifiable from X and the observable F_f , that is, there is a unique function β yielding the model observable F_f .*

Proof. The reformulated problem (18) is given by

$$F_f(t) = [\beta(X) * (f(X) + F_f)](t).$$

This is a Volterra integral equation of the first kind for $\beta(X)$. A classical result (e.g. [20]) states that this equation has a unique solution under the conditions

- $F_f \in C^1$ with $F_f(0) = 0$
- $F_f + f(X) \in C^1$ with $[F_f + f(X)](0) \neq 0$.

These conditions hold under the assumptions in the statement of the corollary. □

3.2 Reformulation for metastatic generations

Eqs. (12-13) can also be reformulated into integral equations for the observables. Let $F_f^k := \int_1^b f(x)\rho^k(x,t)dx$ be the observable associated to the k -th metastatic generation. The previous proof can easily be adapted to show that F_f^0 is given by

$$F_f^0(t) = [f(X) * \beta(x_p)](t) \tag{20}$$

and that for $k \geq 1$, F_f^k is given by

$$F_f^k(t) = [\beta(X) * F_f^{k-1}](t). \tag{21}$$

3.3 Reformulation in the 2D model

Theorem 2. *Let ρ be the solution of the 2D model (14), X_p the primary tumour size and for given σ , and $X(\cdot; \sigma)$ the solution of (16). Then, the observable*

$$F_f(t) = \int_{\Omega} f(x, y) \rho(x, y, t) dx dy$$

is solution of the Volterra equation of the second kind of convolution type

$$F_f(t) = [\Psi(f) * \beta(x_p)](t) + [\Psi(\beta) * F_f](t), \quad (22)$$

where

$$\Psi(h)(t) := \int_{\partial\Omega} N(\sigma) h(X(t; \sigma)) d\sigma \quad (23)$$

Proof. We recall the conservation property (17) of the two-dimensional transport equation:

$$\frac{d}{dt} (\rho(X(t; \sigma), t) J_{\Phi}(t; \sigma)) \equiv 0.$$

Using the change of variables $X = X(s; \sigma)$, $dX = J_{\Phi}(X(s)) ds$, we have

$$\begin{aligned} F_f(t) &= \int_0^t \int_{\partial\Omega} f(X(\tau; \sigma)) J_{\Phi}(\tau, \sigma) \rho(X(\tau; \sigma), t) d\sigma d\tau \\ &\stackrel{(17)}{=} \int_0^t \int_{\partial\Omega} f(X(\tau; \sigma)) (G \cdot \nu)(\sigma) \rho(\sigma, t - \tau) d\sigma d\tau \\ &\stackrel{(14)}{=} \int_0^t \int_{\partial\Omega} f(X(\tau; \sigma)) N(\sigma) \left(\beta(X_p(t - \tau)) + \int_{\Omega} \beta(X) \rho(X, t - \tau) dX \right) d\sigma d\tau \\ &= \int_0^t b(f)(\tau) \left(\beta(X_p(t - \tau)) + \int_{\Omega} \beta(X) \rho(X, t - \tau) dX \right) d\tau \\ &= \Psi(f) * (\beta(X_p) + F_{\beta})(t), \end{aligned} \quad (24)$$

with $\Psi(f)$ defined as in (23). Eq. 24 yields (22) for F_{β} and this can be used to obtain the general result exactly as in the 1D case. \square

Remark 6 (Independent traits of newborn metastases). *Note that hypothesis (15) is also crucial for the model reformulation into a Volterra integral equation of convolution type.*

4 Comparing the efficiency of the PDE-based and the IE-based resolution schemes

In this section, we will show that the calculation of the observables of models (1-4), (12-13) and (14) is much more efficient when starting from the reformulation into the corresponding integral equations (18), (20-21) and (22). Generally speaking, the numerical gain is due to four factors:

1. Better constants in error estimates (generational and full models),
2. High-order quadrature by Newton-Cotes formulas is possible for the IE-based but not for the PDE-based formulation; the discretisation steps of the latter come from the characteristic scheme and are therefore non-uniform (generational model),
3. Availability of additional efficient numerical integration methods for Volterra integral equations (full model),
4. Use of the *Fast Fourier Transform* in the parallel computation of convolutions (generational and full models).

In the following, these factors will be illustrated numerically. A more detailed, heuristic discussion of the constants in error estimates can be found in Appendix A. It should be mentioned that points (1) and (2) can also be achieved by transforming the size-structured model into an age-structured one. This was done by Benzekry [6], although the numerical advantages have not been described. This transformation can actually be seen as the first step in the reformulation as a Volterra integral equation.

4.1 Numerical results, 1D

Setting In this section, we will compare the two 1D model formulations numerically in two scenarios:

A clinical scenario Iwata *et al.* [19] estimated parameters in model (1-4) from a clinical case with the parametrisation explained in Section 2:

$$a = 2.86 \cdot 10^{-3}, b = 7.3 \cdot 10^{10}, x_0 = 1, m = 5.3 \cdot 10^{-8}, \alpha = 0.663.$$

The observation timescale typically being several years, we will take an observation timepoint 1000 days after primary tumour inception.

A preclinical scenario In a murine model with xenografted tumour cells, the parameters have a different order of magnitude. We take

$$a = 0.08, b = 6 \cdot 10^8, x_0 = 5 \cdot 10^4, m = 10^{-5}, \alpha = 2/3$$

(based on unpublished data which will be discussed in [15]). A typical observation timescale is of 40-80 days. We will take an observation timepoint 64 days after primary tumour xenograft.

We will compare the computation of the metastatic mass $M(t) = \int_1^b x\rho(x,t)dx$. Note that if one wants to calculate several observables at the same time, the technique described in Section 5 permits to calculate the whole metastatic density $\rho(\cdot, T)$ efficiently, which can then be used to calculate any observable. In view of statistical parameter estimation as an application, we have chosen a single observation timepoint rather than the whole discrete grid because the

number of observations per individual would be expected to be low. To illustrate the differences between the two model formulations more clearly, the layers of model complexity are added one at a time. Note that due to reasons that will be explained in the following, some tests are not presented in every scenario.

Primary tumour emission Let us start with the simplest model formulation, that is, metastatic emission by the primary tumour only (Eqs. 12 and 20). We will compare first, second and fourth order quadrature formula for the two model formulations. Since an exact calculation of the characteristic curves is possible for the Gompertz growth model, the convergence order is determined by the quadrature order. In a more general case, the order of convergence would also depend on the order of the characteristics calculation. The fourth-order quadrature of the IE version is done with a Newton-Cotes formula (Simpson’s rule). The size discretisation of the PDE version depending on the non-uniform discretisation of the characteristic scheme, a fourth-order PDE-based quadrature must be done differently. With “Gaussian” weights calculated from the discrete points x_i in a way that the quadrature is exact for polynomials up to third order, a fourth order quadrature of the metastatic mass can be achieved. The number of points needed for fourth order quadrature is three in the IE version and four in the PDE version.

Fourth order quadrature is not shown in the clinical scenario because the large scale differences result in numerical instabilities of the PDE-based method when determining the Gaussian weights, which degrades convergence and makes computation times uncomparable. Relative errors are compared in Figure 2, and computation times in Figure 3.

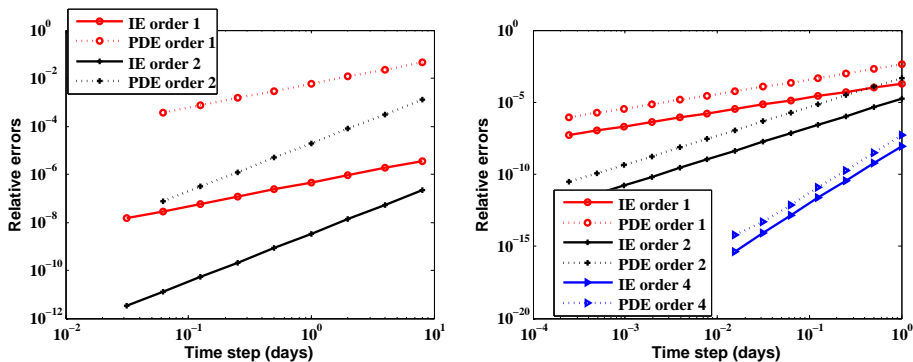


Figure 2: *Relative errors for calculation of the metastatic mass in the one-generational model. Left: clinical scenario, right: preclinical scenario. For both scenarios and any order of quadrature, error constants are considerably better for the IE-based methods.*

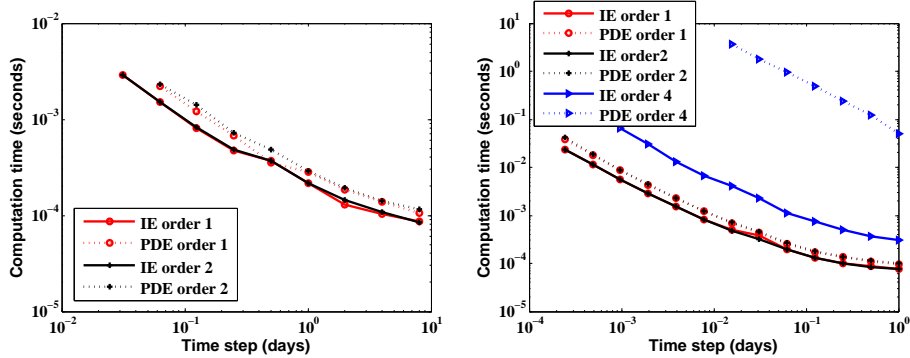


Figure 3: Calculation times for the metastatic mass in the one-generational model. Left: clinical scenario, right: preclinical scenario. For first and second order quadrature, calculation times are slightly inferior for the IE-based models (approx. 20 % less). Calculation times for fourth order quadrature are distinct by several orders of magnitude because the PDE-based method involves the computation of Gaussian weights, which makes it structurally much more complex than the corresponding IE-based method.

Metastatic generations We will now compare the two approaches in a two-generation setting (Eqs. (12-13) and (20-21) with $k = 1$). From this point onwards, a considerable gain in calculation time can be obtained by a FFT-based calculation of the IE-based metastatic mass. Although we are only interested in calculating the observable at one timepoint, the previous generation has to be evaluated at all timepoints prior to the observation time, hence the interest of a fast parallel convolution calculation by FFT.

Errors are compared in Figure 4, and calculation times in Figure 5. Due to the high computational cost of the Gaussian weights, the fourth-order PDE-based quadrature is unfeasible in both scenarios and has been omitted. However, an efficient fourth order IE-based calculation is possible, and even though it is not displayed here as it lacks its PDE counterpart, it will be used in a later section when discussing the convergence of the generational model to the full model.

Full metastatic model The full metastatic model formulations are given by Eqs. (1-4) and (18), respectively. A major advantage of the IE formulation of the full model is that an extension of the classical Runge-Kutta theory to Volterra integral equations can be used for resolution (see [23] and [8]). In addition to that, efficient techniques have been developed to exploit the FFT for the resolution of Volterra integral equations of convolution type. As an example, Hairer *et al.* [14] describe an algorithm computing the solution of a Volterra integral equation of convolution type discretised by an extended Runge-Kutta method in $\mathcal{O}(N \log(N)^2)$ complexity. In our comparison of the two model formulations,

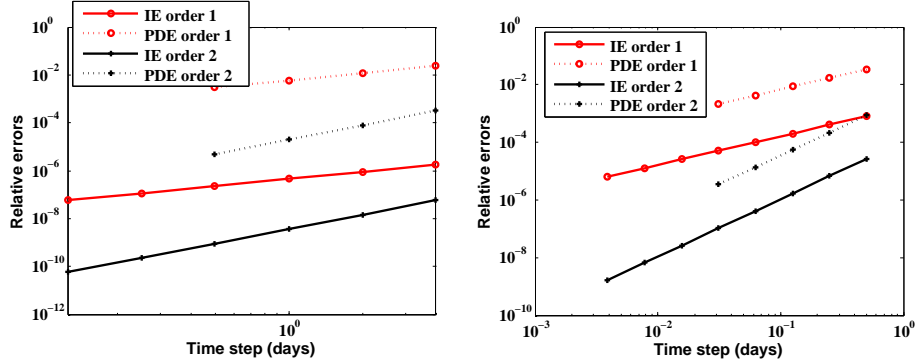


Figure 4: *Relative errors for the computation of the metastatic mass in the two-generational model. Left: clinical scenario, right: preclinical scenario. Again, for both scenarios and any order of quadrature, error constants are considerably better for the IE-based methods.*

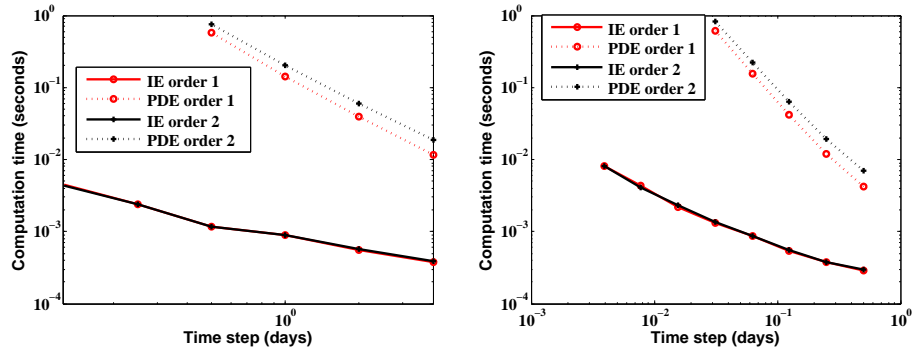


Figure 5: *Calculation times for the metastatic mass in the two-generational model. Left: clinical scenario, right: preclinical scenario. The FFT-based calculation of the IE-based metastatic mass permits a resolution with a $\mathcal{O}(N \log(N))$, opposed to a $\mathcal{O}(N^2)$ complexity of the PDE-based resolution. Note that the PDE-based resolution of the two-generational model is as complex as that of the full model. The PDE-based two-generational metastatic mass is only computed for comparison with the IE-based version.*

this algorithm has been used for the resolution of models (18) and (22). It should be noted that this method has been chosen for illustrative purposes only, and that we do not suggest that it is the best possible way of solving the reformulated problem. An extensive discussion of the different numerical methods for the resolution of Volterra integral equations of convolution type is beyond the scope of this work.

Relative errors are compared in Figure 6, and computation times are the object of Figure 7).

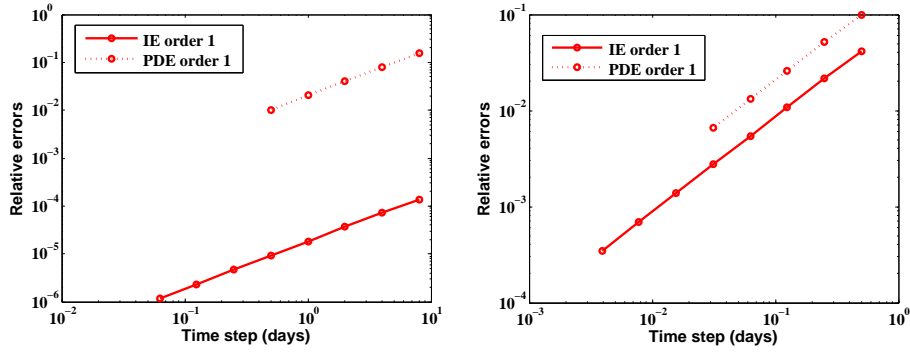


Figure 6: *Relative errors for calculation of the metastatic mass in the full model. Left: clinical scenario, right: preclinical scenario. For both scenarios, error constants are considerably better for the IE-based methods.*

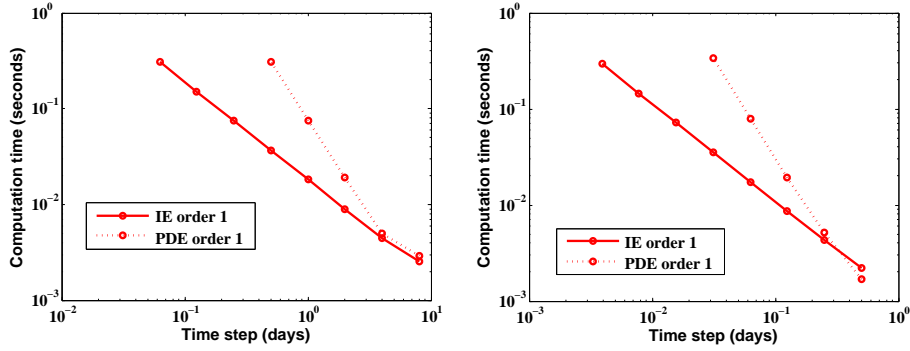


Figure 7: *Calculation times for the metastatic mass in the full model. Left: clinical scenario, right: preclinical scenario. For intermediate and small discretisation steps, the IE-based resolution is more time efficient ($O(N \log(N)^2)$ complexity) than the PDE-based resolution ($O(N^2)$ complexity).*

Convergence of metastatic generations to the full model Depending on the timescale, the generational model can even be efficient for approximation of the full metastatic model. This is due to two factors:

- The calculation of a small number of metastatic generations is faster than the resolution of the full model,
- The error constants appearing in the generational models are better than those appearing in the full model. This is due to the fact that the full model method is explicit while the generational model uses previous generations at all times.

For a given precision of the calculation to be attained, and up to a certain limit observation time, the generational model will therefore be the most efficient way to approximate the full model (see Table 1).

T_{obs}	#G	t_{gen}	t_{full}	gain	T_{obs}	#G	t_{gen}	t_{full}	gain
1 years	2	0.01	0.5	50	2 weeks	2	0.001	0.02	23
2 years	2	0.02	1.1	50	4 weeks	3	0.002	0.04	18
3 years	3	0.1	2.1	20	6 weeks	4	0.007	0.07	12
4 years	4	0.2	2.1	10	8 weeks	5	0.01	0.07	5
5 years	4	0.2	2.1	10	10 weeks	5	0.03	0.13	5

Table 1: *Left: clinical parameters, right: preclinical parameters. T_{obs} =observation time, #G=minimal number of generations needed for attaining the relative precision 10^{-8} . t_{gen} =calculation time of #G-generational model in seconds, t_{full} =calculation time of full model in seconds, gain = $\frac{t_{full}}{t_{gen}}$. Fourth order methods have been used to solve the generational and full models. Time discretisation steps have been chosen such that the quadrature errors are near machine error (much smaller than 10^{-8}). It is thus the difference between generational and full models that is compared to the precision 10^{-8} , and not the approximation errors.*

Remark 7. *The high-order approximation of the full model by metastatic generations has practical limitations. Taking Simpson's rule as an example, the fourth-order calculation of generation k on a grid with size Δt requires that generation $k - 1$ be evaluated on a grid with size $\frac{\Delta t}{2}$. Thus, in a k -generational model, the very first generation has to be evaluated on a grid with size $\frac{\Delta t}{2^{k-1}}$, which will only be precise up to machine precision if k is large. This error propagates and deteriorates the precision of the calculation of generation k . This leads to an decrease of the attainable precision by generational approximation.*

4.2 Numerical results, 2D

Preclinical setting In this section, we will compare the two 2D model formulations numerically in the following preclinical scenario, with parameters in

g and β taken from Benzekry *et al.* [7]. Growth is modelled by the Hahnfeldt model [13] describing the evolution of tumour size x and carrying capacity k :

$$g(x, k) = \begin{pmatrix} ax \log(k/x) \\ cx - dx^{2/3}k \end{pmatrix}$$

with the parametrisation $a = 0.154, c = 16.7, d = 0.0717, x_p(0) = 0.1, x_m(0) = 10^{-6}, k_p(0) = 200, k_m(0) = 1$. A rectangular domain $\Omega = (0, b) \times (0, b), b = (c/d)^{3/2}$, can be chosen. Note that size is measured in mm^3 and not in cell numbers. For example, metastases are born with size 10^{-6} , roughly corresponding to the dimension of one cell. Emission depends only on size and not on carrying capacity, that is, $\beta(x, k) = mx^\alpha$ with $m = 0.0229, \alpha = 2/3$. Note that there is an indirect link between carrying capacity and emission through the fact that tumour size is driven towards the carrying capacity in the Hahnfeldt Model. Benzekry *et al.* supposed that the initial carrying capacity is the same for all metastases ($N(\sigma) = \delta_{k_m(0)}$). However, in order to have a true 2D model as a benchmark for the numerical methods, we will assume that metastases are born with a random initial carrying capacity between 0.8 and 1.2 (that is, according to $N(\sigma) = 2.5 \cdot \chi_{[0.8, 1.2]}(\sigma)$).

Results for the full 2D model A similar numerical gain as in the 1D model is obtained in the 2D case. We will therefore restrict ourselves to describe the major difference only appearing in the 2D model. Let us suppose that we discretise Eqs. 14 and Eq. 22 with N steps in time and K steps on the boundary. In the PDE method, a 2D integral ($N \cdot K$ complexity) has to be computed **at each timepoint**, which yields a total complexity of $\mathcal{O}(N^2 \cdot K)$. In contrast to this, a 2D quadrature with $\mathcal{O}(N \cdot K)$ complexity is **only needed for the calculation of the source term and the kernel** of the Volterra equation. The Volterra convolution equation is then solved in $\mathcal{O}(N \log(N)^2)$. In the IE formulation, the two processes that were entangled in the PDE formulation are decoupled, yielding in total a $\mathcal{O}(N \cdot K + N \log(N)^2)$ complexity. See Figure 8 for computation times in the previously described setting. Note that the characteristic curves of the Hahnfeldt growth model have to be approximated numerically. Both the calculation time of the 2D quadrature and the error constants depend on the particular method used for this computation, but the gain in structural complexity does not depend on this choice.

5 Extensions and limitations of the reformulation

In this chapter, we will explore the degree of generality of the method discussed in the previous chapters. We will show that the same kind of reformulation can be performed for a non-zero initial condition and for a Dirac-type observable. However, if the action of a treatment is modelled (time-dependence of the growth rate g), the Volterra equation obtained is not of convolution type.

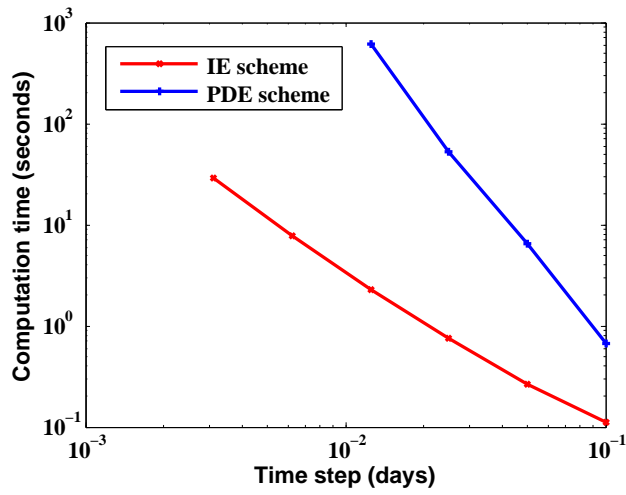


Figure 8: *2D* model calculation times of the metastatic mass in the previously described scenario. The boundary discretisation step ds has been set to $ds = C \cdot dt$, where dt is the time discretisation step and $C = 0.1$. The characteristic curves have been approximated numerically by a first order method. In this setting, the PDE-based resolution has a $\mathcal{O}(N^3)$ complexity, whereas the IE-based resolution only has a $\mathcal{O}(N^2)$ complexity.

5.1 Reformulation for a non-zero initial condition

Lemma 1. *Let ρ be the solution of (7). Then, the observable F_f is solution of the Volterra integral equation of convolution type*

$$F_f = \Psi_f + f(X) * (S + \Psi_\beta) - \beta(X) * \Psi_f + \beta(X) * F_f, \quad (25)$$

where $\Psi_h(t) := \int_1^b h(X(X^{-1}(x) + t))\Phi(x)dx$.

Proof. We split the integral into two parts:

$$F_f(t) = \int_1^{X(t)} f(x)\rho(x, t)dx + \int_{X(t)}^b f(x)\rho(x, t)dx.$$

In the first term, which we will denote $F_f^1(t)$, the characteristics come from the boundary $[0, t]$. Therefore, the same manipulation as in Theorem 1 can be done here, yielding

$$F_f^1(t) = [f(X) * (S + F_\beta)](t).$$

The characteristics in the second term, denoted $F_f^2(t)$, come from the initial condition:

$$\begin{aligned} F_f^2(t) &= \int_t^{+\infty} f(X(s))g(X(s))\rho(X(s), t)ds \\ &= \int_0^{+\infty} f(X(s+t))g(X(s))\rho(X(s), 0)ds = \Psi_f(t). \end{aligned}$$

Summing up the two terms, we obtain

$$F_f(t) = [f(X) * (S + F_\beta)](t) + \Psi_f(t).$$

The technique used in the proof of Theorems 1 and 2 permits to conclude. \square

5.2 Efficient calculation of the metastatic density function

ρ

Up to now, the focus has been on biological observables of the form $F_f(t) = \int_1^b f(x)\rho(x, t)dx$. However, the reformulation can also be used for a more efficient calculation of the whole metastatic density $\rho(\cdot, T)$ for a fixed time T .

First of all, Remark 3 will not be sufficient to justify the reasoning that will follow. We will need a stronger regularity result, which is given in the Appendix. That being said, the Volterra integral equation established for the rate of metastatic birth $F_{birth}(t) := g(1)\rho(1, t)$ is given by

$$F_{birth}(t) = \beta(x_p(t)) + (\beta(X) * F_{birth})(t)$$

which can be solved on $[0, T]$ with efficient FFT-based methods as shown in Chapter 4. The improved regularity result then permits to follow the characteristics using the conservation property (10) to calculate $\rho(\cdot, T)$.

5.3 No convolution equation in the non-autonomous case

If the growth term g depends on the time, as would be the case for modelling a therapy (see [26] in 1D and [5] in 2D), it is still possible to formulate F_β as the solution of a Volterra integral equation. The conservation relation changes to

$$\frac{d}{dt}\rho(t, X(t; t_0, x_0)) = \rho(t, X(t; t_0, x_0))\partial_x g(t, X(t; t_0, x_0))$$

and therefore

$$\rho(t, X(t; t_0, x_0)) = \rho(x_0, t_0) \cdot \exp\left(-\int_{t_0}^t \partial_x g(s, X(s; x_0, t_0))\right).$$

We perform the reformulation as previously:

$$\begin{aligned} F_f(t) &= \int_0^t f(X(t; s, 1))g(s, X(t; s, 1))\rho(s, 1)e^{-\int_s^t \partial_x g(\tau, X(\tau; s, 1))d\tau} ds \\ &= \int_0^t k(t, s)(S(s) + F_\beta(s))ds, \end{aligned}$$

denoting

$$k(t, s) := \frac{1}{g(s, 1)}f(X(t; s, 1))g(s, X(t; s, 1))e^{-\int_s^t \partial_x g(\tau, X(\tau; s, 1))d\tau}.$$

For $f = \beta$, this yields the Volterra integral equation

$$F_\beta(t) = \int_0^t k(t, s)(S(s) + F_\beta(s))ds.$$

Unfortunately, the equation is not of convolution type anymore, and for general f , F_f cannot be written in this way.

Note that while an FFT-based calculation of F_β is not possible if the Volterra integral equation is not of convolution type, efficient quadrature techniques (such as extended Runge-Kutta methods, see Section 4) can be applied to Volterra integral equations with general kernels. A comparison of the numerical performance of the IE versus the PDE formulation in case of non-autonomous growth rates could yield interesting insights but is beyond the scope of this article.

6 Conclusion

In this article, we have proposed a model reformulation applicable to a family of 1D and 2D metastatic growth models, which has been shown to improve the numerical resolution substantially.

In the literature, the metastatic models considered in this work have been described as PDE for a metastatic density function. However, the quantities of interest are often not the density itself but rather biologically relevant quantities such as the number of metastases or the metastatic mass, which can be

written as weighted integrals of the metastatic density. To begin with, we have formulated these model observables as solutions of Volterra integral equations of convolution type. Special attention had to be paid to regularity of solutions and an improved regularity result has been proven. The reformulated model permitted to tackle an analytical problem, structural identifiability of the 1D model.

We have then compared the two model versions thoroughly in terms of numerical resolution efficiency. Three scenarios with parameters estimated from clinical and preclinical data have been taken as model benchmarks. Apart from the full model, a generational formulation has been discussed. For all test cases and models versions, the resolution of the reformulated model has been shown to be both more precise and faster. There are four reasons for this numerical gain, namely better error constants, better quadrature formulas, availability of additional efficient numerical integration methods, and use of the *Fast Fourier Transform*. The fact that much better error constants are obtained is far from trivial. We have therefore discussed this result heuristically in a more general framework, characteristic of tumour growth dynamics.

An accelerated resolution of the metastatic growth models has a direct application in statistical parameter estimation, where large numbers of model evaluations are needed. In this framework, the IE-based model resolution can make statistical approaches feasible which would not be possible in the PDE-based model.

The performance of generational models has been a major focus in this article. Apart from the approximation of the full model, generational models will in many cases be the most efficient way of estimating parameters from data. Typically, only the first few metastatic generations (i.e., one or two) will have an impact on the parameter estimates. Roughly speaking, this is because the model error (full vs. generational) soon becomes negligible compared to the measurement error.

The crucial hypothesis for obtaining a convolution structure in the Volterra integral equation is an autonomous metastatic growth rate g . When estimating parameters in a treatment scenario, this assumption will no longer hold. We have shown that a non-convolution type Volterra integral equation can be obtained for the observable F_β , which can then be used to calculate arbitrary observables. Although the numerical gain will certainly be less prominent than in the autonomous case, the availability of efficient numerical methods for the reformulated model, such as extended Runge-Kutta schemes, might in itself improve the numerical resolution. Future works will clarify this question.

A Heuristic explanation of the improvement in error constants in the IE-based model resolution

In this section, we will discuss the observation that the error constants obtained in the IE-based model resolution are much better than those of the PDE-based model resolution (the first of four factors evoked at the beginning of Section 4). We will take a more general framework, characteristic of tumour growth dynamics, and use heuristic arguments.

We will consider the two (explicit) formulations of the metastatic mass in the one-generation metastatic model (Eqs. (12) and (20), respectively) calculated with a rectangle rule:

$$M_{IE}(t_n) = \Delta t \sum_{i=1}^n \beta(x_p(t_{n-i}))X(t_i),$$

$$M_{PDE}(t_n) = \sum_{i=1}^n \frac{X(t_i) - X(t_{i-1})}{g(X(t_i))} \beta(x_p(t_{n-i}))X(t_i).$$

The first order error terms are given by

$$|(M - M_{IE})(t_n)| = \frac{\Delta t}{2} |x_n \beta(x_p(0)) - \beta(x_p(t_n))|,$$

$$|(M - M_{PDE})(t_n)| = \frac{\Delta t}{2} \left| x_n \beta(x_p(0)) - \beta(x_p(t_n)) + \int_0^{t_n} g'(X(s))X(s)\beta(x_p(t_n - s))ds \right|.$$

These error terms can be calculated explicitly if $x_p(t) = X(t) = x_0 e^{at}$ and $\beta(x) = mx^{2/3}$, yielding:

$$|M(t_n) - M_{PDE}(t_n)| = 2|M(t_n) - M_{IE}(t_n)|. \quad (26)$$

Also, in the case $x_p(t) = X(t) = (1 + at)^2$ and $\beta(x) = mx^{2/3}$, the asymptotical result

$$|M(t_n) - M_{PDE}(t_n)| \approx ct_n^{4/3} |M(t_n) - M_{IE}(t_n)| \quad (27)$$

can be obtained.

As tumour growth model as the Gompertz model exhibit an exponential growth phase at the beginning, (26) gives a good description of the errors for short time intervals. Tumour growth subsequently decelerates, which leads to an increase in the PDE error term that is superior to that of the IE error term, much like in (27).

B Regularity of the solution of Eqs. (1-4).

Lemma 2 (Regularity of ρ). *Let $T > 0$, $S \in C^1([0, T])$, $\Phi \in C^1([1, b])$ with $\Phi(b) = 0$ and $g \in C^1([1, b])$ positive and with $g(b) = 0$. Then, the unique weak*

solution $\rho \in C([0, T], L^1(1, b))$ of (7) is continuously differentiable on the two domains separated by the solution of (6), that is, on

$$\begin{aligned}\Omega^+ &:= \{(x, t) \in [1, b) \times [0, T] : x < X(t)\}, \\ \Omega^- &:= \{(x, t) \in [1, b) \times [0, T] : x > X(t)\}.\end{aligned}$$

Proof. We will proceed along the lines of the proof of existence of strong solutions by Barbolosi *et al.* [2]. The main difficulty arising in Lemma 2 is that condition (9) is not assumed, leading to a discontinuity of ρ along X . Thus, the solution ρ has to be constructed on both subdomains Ω^+ and Ω^- separately. Let us first consider the case $\Phi \equiv 0$ and define $\Omega^+(\tau_1, \tau_2) := \Omega^+ \cap (1, b) \times (\tau_1, \tau_2)$ and

$$\mathcal{X}(\tau_1, \tau_2) := \left\{ w \in C^1(\overline{\Omega^+(\tau_1, \tau_2)}) : g(1)w(1, \tau_1) = S(\tau_1) + \int_1^{X(\tau_1)} \beta(y)w(y, \tau_1)dy \right\},$$

which, endowed with the C^1 norm, is a Banach space. Let $\mathcal{X} := \mathcal{X}(0, T_1)$ with T_1 to be determined in the following and let \mathcal{F} be the function that maps $w \in \mathcal{X}$ on the solution ρ of

$$\begin{aligned}\partial_t \rho(x, t) + \partial_x [g(x)\rho(x, t)] &= 0, \\ g(1)\rho(1, t) &= S(t) + \int_1^{X(t)} \beta(x)w(x, t)dx.\end{aligned}$$

As Barbolosi *et al.*, we will construct a fixed point solution of \mathcal{F} by showing that $\mathcal{F} : \mathcal{X} \rightarrow \mathcal{X}$ and that for T_1 sufficiently small, \mathcal{F} is a contraction. The compatibility condition $g(1)\mathcal{F}(w)(1, 0) = S(0)$ holds by definition of $\mathcal{F}(w)$. The explicit formulation

$$\mathcal{F}(w)(x, t) = \frac{1}{g(x)} \left(f(t - X^{-1}(x)) + \int_1^{X(t - X^{-1}(x))} \beta(y)w(y, t - X^{-1}(x))dy \right),$$

obtained with the conservation property along the characteristics, can be used to show that $\mathcal{F}(w) \in \mathcal{X}$ and that

$$\|\mathcal{F}(w_1) - \mathcal{F}(w_2)\|_{\mathcal{X}} \leq C_T \cdot T_1 \cdot \|w_1 - w_2\|_{\mathcal{X}}.$$

Choosing $T_1 = \frac{1}{2 \cdot C_T}$, the contraction property is shown. As in Barbolosi *et al.*, for arbitrarily large times a bootstrap argument can be used. The solutions obtained on the subdomains can be “glued” together into a function $\tilde{\rho} \in C^1(\Omega^+)$. It can now be shown that

$$\rho = \begin{cases} \tilde{\rho} & \text{on } \Omega^+ \\ 0 & \text{on } \Omega^- \end{cases}$$

is a weak solution of problem (7) by simply integrating by parts on each subdomain. Note that no additional term appears on the boundary separating Ω^+ and Ω^- because the flux is always parallel to the boundary.

In the case $\Phi \neq 0$, we use the following argument. On Ω^- , the solution ρ can be written explicitly as

$$\rho(x, t) = \frac{g(X(X^{-1}(x) - t))}{g(x)} \Phi(X(X^{-1}(x) - t)),$$

which is a C^1 function if Φ is C^1 . The integral term appearing in the boundary condition can now be split into two terms. The part in Ω^- acts as an additional (regular) source term, and what remains can be dealt with as previously. \square

Acknowledgment

The author would like to thank Florence Hubert, Sebastien Benzekry and Assia Benabdallah for useful discussions and propositions. The author was partially supported by the Agence Nationale de la Recherche under grant ANR-09-BLAN-0217-01 and by the Cancéropôle PACA.

References

- [1] C.H.T. Baker. A perspective on the numerical treatment of Volterra equations. *J Comput Appl Math*, 125:217–249, 2000.
- [2] D. Barbolosi, F. Verga, A. Benabdallah, and F. Hubert. Mathematical and numerical analysis for a model of growing metastatic tumors. *Math Biosci*, 218(1):1–14, 2009.
- [3] D. Barbolosi, F. Verga, B. You, A. Benabdallah, F. Hubert, C. Mercier, J. Ciccolini, and C Faivre. Modélisation du risque dévolution métastatique chez les patients supposés avoir une maladie localisée. *Oncologie*, 13(8):528–533, 2011.
- [4] S. Benzekry. Mathematical analysis of a two-dimensional population model of metastatic growth including angiogenesis. *J Evol Equ*, 11(1):187–213, 2011.
- [5] S. Benzekry. *Modélisation et analyse mathématique de thérapies anti-cancéreuses pour les cancers métastatiques*. PhD thesis, Aix-Marseille Université, 2011.
- [6] S. Benzekry. Mathematical and numerical analysis of a model for anti-angiogenic therapy in metastatic cancers. *ESAIM-Math Model Num*, 46(2):207–237, 2012.
- [7] S. Benzekry, A. Gandolfi, and P. Hahnfeldt. Global Dormancy of Metastases due to Systemic Inhibition of Angiogenesis. Submitted.
- [8] H. Brunner, E. Hairer, and S.P. Nørsett. Runge-Kutta theory for Volterra integral equations of the second kind. *Math Comp*, 39:147–163, 1982.

- [9] C. L. Chaffer and R. A. Weinberg. A perspective on cancer cell metastasis. *Science*, 331(6024):1559–1564, Mar 2011.
- [10] A. Devys, T. Goudon, and P. Lafitte. A model describing the growth and the size distribution of multiple metastatic tumors. *Discret Contin Dyn S*, 12:731–767, 2009.
- [11] G. P. Gupta and J. Massague. Cancer metastasis: building a framework. *Cell*, 127(4):679–695, Nov 2006.
- [12] M. Gyllenberg and G.F. Webb. Quiescence as an Explanation of Gompertzian Tumor Growth. *Growth Develop Aging*, 53:25–33, 1989.
- [13] P. Hahnfeldt, D. Panigrahy, J. Folkman, and L. Hlatky. Tumor development under angiogenic signaling: a dynamical theory of tumor growth, response and postvascular dormancy. *Cancer Res*, 59:4770–4775, 1999.
- [14] E. Hairer, C. Lubich, and M. Schlichte. Fast numerical solution of nonlinear Volterra convolution equations. *J Sci Stat Comp*, 5:532–541, 1985.
- [15] N. Hartung. Modelling of metastatic growth and *in vivo* imaging. PhD thesis (in preparation).
- [16] N. Hartung, S. Mollard, D. Barbolosi, A. Benabdallah, G. Chapuisat, J. Ciccolini, C. Faivre, S. Giacometti, G. Henry, A. Iliadis, and F. Hubert. Mathematical modeling of tumor growth and metastatic spreading: validation in tumor-bearing mice. Submitted.
- [17] V. Haustein and U. Schumacher. A dynamic model for tumour growth and metastasis formation. *J Clin Bioinforma*, 2(1):11, 2012.
- [18] M. Iannelli. *Mathematical theory of age-structured population dynamics*. Applied Mathematical Monographs, C.N.R.I. Giardini Editori e Stampatori, Pisa, Pisa, 1995.
- [19] K. Iwata, K. Kawasaki, and N. Shigesada. A Dynamical Model for the Growth and Size Distribution of Multiple Metastatic Tumors. *J Theor Biol*, 203:177–186, 2000.
- [20] T. Lalescu. *Introduction à la théorie des équations intégrales. Avec une préface de É. Picard*. A. Hermann et Fils, Paris, 1912.
- [21] A.G. McKendrick. Applications of mathematics to medical problems. *Proc Edinburgh Math Soc*, 44:98–130, 1926.
- [22] B. Perthame. *Transport Equations in Biology*. Frontiers in Mathematics. Birkhäuser Basel, 2007.
- [23] P. Pouzet. Étude en vue de leur traitement numérique des équations intégrales de type Volterra. *Rev Franç Traitement Information Chiffres*, 6:79–112, 1963.

- [24] J.G. Scott, P. Gerlee, D. Basanta, A.G. Fletcher, P.K. Maini, and A.R.A. Anderson. Mathematical modelling of the metastatic process. *Preprint*, 2013.
- [25] A. Stein, D. DeWoskin, M. Higley, K. Lemoi, B. Owens, A. Rahman, H. Rotstein, D. Rumschitzki, S. Swaminathan, M. Tanzy, O. Varfolomiyev, T. Witelski, and V. Zubekov. Dynamic models of metastatic tumor growth. Final Report of the 27th Annual Workshop on Mathematical Problems in Industry, New Jersey Institute of Technology, 2011.
- [26] F. Verga. *Modélisation mathématique de processus métastatiques*. PhD thesis, Aix-Marseille Université, 2010.
- [27] H. Von Foerster. Some remarks on changing populations. In *The Kinetics of Cell Proliferation*, pages 382–407, 1959.